Experimental and Theoretical Study of the Laser Induced Diffraction Pattern in the Acid Orange 10 Dye: Polyacrylamide Gel

Hassan A. Sultan, Hussain A. Badran ,Alaa, Y. Al-Ahmad* and Chassib A. Emshary

Department of Physics, College of Education, University of Basrah, Basrah, Iraq

* Corresponding author

e-mail: alaa_ta2005@yahoo.com, Phone: +00 9647703291910

Abstract:

We observed and studied diffraction rings generated in an Acid Orange 10 dye doped Polyacrylamide gel (AO10: PAA gel) using cw visible laser beam. The number of rings increases almost exponentially with increasing input power and concentration of the samples. The refractive index change, Δn, effective nonlinear refractive index, n_2, variation of thermo-optic coefficient ,dn/dT, figure of merit ,W, and thermal figure of merit ,H, are found to be 0.004788 , 10^{-5} cm^2/Watt, 1.01×10^{-4} 1/^{o}C, 13.7 and 0.45×10^{-4} respectively. The effective nonlinear refractive index, n_2, was determined based on the observed number of rings. This large nonlinearity is attributed to a thermal effect. Theoretical diffraction patterns that agree well with experimental one are generated using a wave theory.

Keywords: Nonlinearity; Thermal effect; Wave theory.

1. *Introduction*

Self-induced index changes in optical media have been investigated extensively in the past in connection with Q- switching and mode locking of lasers and self-focusing or defocusing of laser beams. The mechanisms behind self- induced changes fall into two categories. In the first category, there are several non-resonant mechanisms which have been studied quite extensively in the past in connection with self-focusing. In the second category, we have near-resonant effects, the most important of which is associated with the saturation of a more-or-less homogenously broadened absorption line [1]. A Fréedericksz transition caused by the electric field of wave was first observed by Zolot'ko and colleagues [1]. He and his colleagues published series of articles concerning the appearance of aberration

pattern (rotation of the plane of polarization, time dependences of the intensity of the central spot, and elongation of the aberration rings) formed as a result of self-focusing of a light beam caused by the Fréedericksz transition [2-8]. For various reasons the diffraction pattern in the shape of concentric rings was studied, viz, strong self-defocusing effect and foure-wave mixing in bacteriorhodopsin films [9] absorbing solution [10], optical multistability in nematic liquid crystal [11], organically modified sol-gel materials [12], mercury dithizonate [13], femtosecond Bessel beams [14], self-focusing spatial beams [15] and bulk ceramic and thin film PLZT [16].

There is considerable interest in finding materials having large yet fast nonlinearities. This interest, that is driven primarily by the search for materials for all-optical switching and sensor protection applications, concerns both nonlinear absorption and nonlinear refraction. The database for nonlinear optical properties of materials, particularly organic, is in many cases inadequate for determining the trends to guide synthesis efforts.
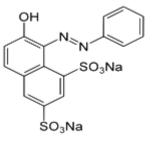
In the present work we present experimental evidences of observing diffraction pattern in acid orange 10 dye: polyacrylamide gel (AO10: PAA gel) together with the calculation of the refractive index change, Δn , effective nonlinear refractive index ,n_2 , variation of thermo-optic coefficient, dn/dT , figure of merit ,W, and thermal figure of merit ,H . Using a well known theoretical model based on wave theory we have reproduced the diffraction patterns. The obtained results fit reasonably the experimental one.

2. *Experimental Methods*
2.1. Preparation of Material and UV-Visible Studies

The samples of AO10: PAA gel were prepared from 7-Hydroxy-8-phenylazo-1,3-naphthalene-disulfonic acid disodium salt, acid orange 10 (AO10) dye, Sigma-Aldrich, and polyacrylamide (PAA), average Molecular Weight Mw =10,000 g/ mol , Sigma-Aldrich by dissolving (1gm, 2.2 mmol/L) AO10 dye in 50 ml distilled water, and (0.1gm, 1.4 mmol/L) PAA dissolved in 50 ml distilled water, then we mixed AO10 dye solution with PAA solution. The mixture was stirred at room temperature (RT) for 50 min. to inter all AO10 dye molecules within polymer chains, then the solution was filtered through 0.2µm syringe filter. After that the solutions of AO10: PAA were mixed, heated (up to 85 ^{o}C) and stirred for (60 min.), then the mixture was cooled to RT to obtain an AO10: PAA gel. The general structure and molecular formula of AO10 dye is illustrated in fig.1.

$C_{16}H_{10}N_2Na_2O_7S_2$

Fig.1. Chemical structure and molecular formula of AO10 dye

The UV-Visible (UV-Vis) spectroscopy has been used to characterize the AO10:PAA gel samples in the spectral range (300-700 nm). The absorbance (A) of

the samples measurements were carried out using Cecil ReflectaScan CE 3055 Reflectance Spectrometer. These measurements were performed at RT . The optical absorption of the AO10: PAA gel samples of two concentrations (0.15 mmol/L & 0.55 mmol/L) have shown an absorption peak (λ_{max}) at 485 nm; the absorption spectra of AO10: PAA gel samples are presented in fig. 2.
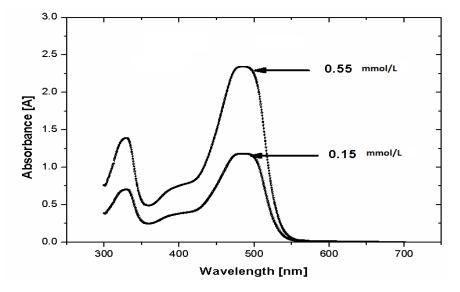

Fig.2. UV–Vis absorption spectrum of two concentrations of AO10: PAA gel of 0.15 and 0.55 mmol /L .

2.2. Experimental Setup

AO10: PAA gel samples at two concentrations of 0.15 and 0.55mmol/L are prepared in a glass cell of 1mm thickness as the nonlinear material in the experiment. The apparatus consists of a diode laser (0-100 mWatt output, beam radius 1.2 mm at $1/e^2$) , a demountable beam splitter , a positive glass lens of +50 mm focal length, a glass cell of 1 mm thickness filled with AO10: PAA gel, a semitransparent screen of 30 cm x30 cm, a digital CCD camera and a detector to measure input power. A stop watch was used to measure nonlinear transmission curve against time in a fixed position for the two concentrations. The output of the CCD camera was fed to a computer for further analysis. A schematic diagram of the experimental setup is shown in fig. 3.
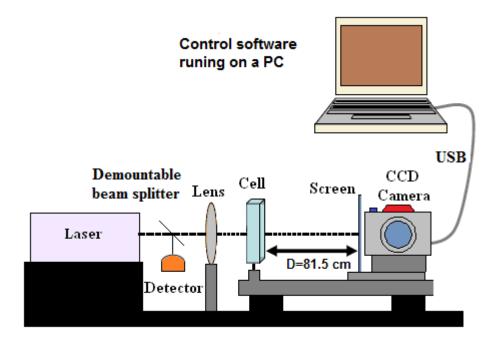
Fig.3. Schematic diagram of the experimental setup

3. Experimental Results
3.1. Diffraction ring patterns

The sample was positioned at or immediately behind the focal point of the lens. As the power was gradually increased, diffraction ring patterns were observed on the screen. Figures 4 and 5 show the observed ring pattern for the 0.15 and 0.55mmol/L concentrations of AO10: PAA gel, respectively, as a function of input power with intensity distribution for each case (i.e x and y distributions of intensity show the complex characteristics of the distribution). The transmitted beam profiles and the distribution of intensity corresponding to the laser input power of 20, 40, 80, and 100 mW are shown.
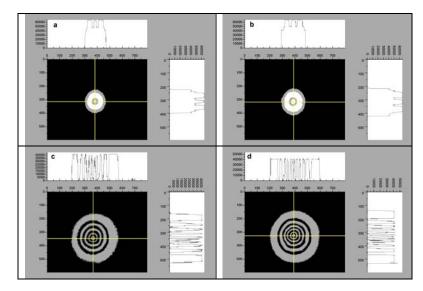

Fig.4. Transmitted beam profiles corresponding to the input power: (a) 20 mWatt, (b) 40 mWatt, (c) 80 mWatt and (d)100 mWatt for 0.15 mmol/L concentration of AO10: PAA gel.

Fig.5. Transmitted beam profiles corresponding to input power : (a) 20 mWatt, (b) 40 mWatt, (c) 80 mWatt and (d)100 mWatt for 0.55 mmol/L concentration of AO10: PAA gel.

3.2. Nonlinear refractive index

The maximum number of rings obtained (9) was for input power 100 mW. We can estimate the induced refractive index change, Δn, and the effective nonlinear refractive index, n_2, for the preceding data as follows. Because the laser beam used in the experiment has a Gaussian distribution, the relative phase shift, $\Delta\varphi$, suffered by the beam while traversing the sample of thickness (L) can be written as [10]:

$$\Delta\varphi = kL\Delta n \qquad (1)$$

Where $k=2\pi/\lambda$ is the wave vector in vacuum and λ is the laser beam wavelength. The relationship between $\Delta\varphi$ and number of rings, N, can be written as [10]:

$$\Delta\varphi = 2\pi N \qquad (2)$$

The relationship between the total refractive index, n, and nonlinear part of the refractive index, n_2, can be written as follows [17]:

$$n = n_0 + \frac{n_2}{2}I$$
$$n = n_0 + \Delta n \qquad (3)$$

Where n_0 is the background refractive index, and I is the laser beam intensity.

The approximate radius of the beam at the sample is $\omega_p=20.28\mu m$, N=9, $\lambda=532nm$, power input 100 mW, sample thickness L=1mm. These numericals lead to the induced refractive change $\Delta n=0.004788$ and the nonlinear refractive index $n_2=10^{-5}$ cm^2 /W. The relation between N, Δn and input power are shown in Fig.6 and 7 .

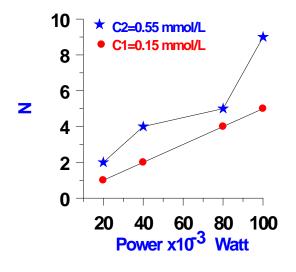**Fig.6. Input power versus N for different.**
concentrations

Fig.7 Input power versus Δn for different
concentrations

The high nonlinear optical refractive index compares favourably with that of some representative of third-order nonlinear optical materials, namely, pararosanilin dye in liquid and solid media [18], basic green 1 dye in aqueous solutions [19], oxazine (OX720) and oxazine (OX750) dye in aqueous solutions and in PAA matrix [20], photo polymerizable organo siloxane [21], and organic polymers [22]. These results predict that AO10: PAA gel has potential applications for nonlinear optics. For practical use in all-optical switching devices many considerations have been taken into account to investigate the effectiveness of nonlinear materials. The figure of merit, *W*, has to be satisfied for 2π

phase shift to evaluate its application in such devices [23]

$$W = \frac{\Delta n_{max}}{\alpha \lambda} > 1 \qquad (4)$$

Where Δn_{max} is the highest change in the value of refractive index obtained at 532 nm.

Under 532 nm excitation, for linear absorption coefficient α= 6.561/cm of AO10: PAA gel, *W*= 13.7 which indicates that the nonlinear optical properties of AO10: PAA gel are sufficient for applications in all-optical switching technology. This high value of figure of merit and large nonlinear refraction makes AO10: PAA gel promising for use in all-optical switching devices.

4. *Theoretical Model of the Diffraction Ring Patterns and Results*

The laser beam used in the present work has a Gaussian extent of wavelength λ. Assuming that the beam propagate along the z-direction and the medium have a length of L with a linear absorption

$$E(r,z) = E(0, z_o) \exp\left[\frac{-r^2}{\omega_p^2}\right] \exp\left[\frac{-ik_o n_o r^2}{2R}\right] \qquad (5)$$

where r is the radial coordinate, z_o is the coordinate position of the medium, k_o (=$2\pi/\lambda$) is the free space wave vector, n_o is the air surrounding the medium refractive index, ω_p is the beam waist at the medium
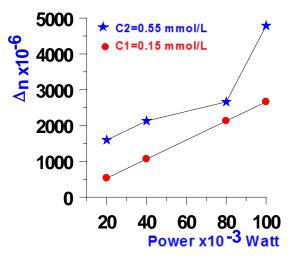
coefficient α. At the entrance of the medium which is taken as the origin of the Cartesian coordinates the electric field of the incident laser beam can be written as [24]:

entrance and R the radius of curvature of its wave-front in the corresponding position.
By taking into account the total phase shift, φ, suffered by the beam during the course of traversing through the medium, the far-

field distribution pattern can be obtained considering the free propagation of the optical wave through space, by means of

Fraunhofer approximation of the Fresnel-Kirchhoff diffraction integral as [24] :

$$I(\rho) = I_o \left| \int_0^\infty J_o(k_o\theta r) \exp\left[-\frac{r^2}{\omega_p^2} - i\varphi(r) \right] r dr \right|^2 \qquad (6)$$

Where $J_o(x)$ is the zero-order Bessel function of the first kind, θ is the far field diffraction angle, ρ is the radial coordinate in the far field observation plane and the intensity I_o can be written as [24]:

$$I_o = 4\pi^2 \left| \frac{E(0, z_o) \exp(-\alpha L/2)}{i\lambda D} \right|^2 \qquad (7)$$

D is related to the radial coordinate by $\rho = D\theta$.

   Using the values of the various parameters given in table1 and solving equation 6, we have generated the theoretical results of diffraction pattern shown in fig. 8 for the four chosen input powers.

Table1. Measured and calculated values of the parameters used to generate fig.8.
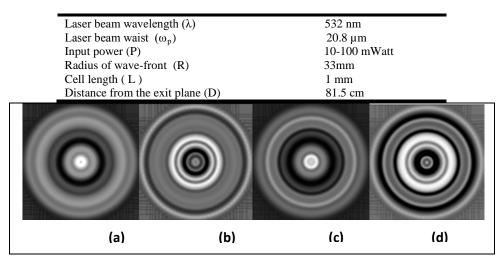
Parameter	Value
Laser beam wavelength (λ)	532 nm
Laser beam waist (ω_p)	20.8 µm
Input power (P)	10-100 mWatt
Radius of wave-front (R)	33mm
Cell length (L)	1 mm
Distance from the exit plane (D)	81.5 cm

(a)   **(b)**   **(c)**   **(d)**

Fig.8. Theoretical results of the diffraction patterns: (a) P=20 mWatt, (b) P=40 mWatt, (c) P=80 mWatt and (d) P=100 mWatt.

5. Thermal Effect Physical Mechanism

   In both cases (figs.4&5) the number of rings increases with increasing input power. The number of rings depends on the concentration too, that is, increasing the concentration increases the number of rings for the same input power. This means that, in the investigated samples, thermal effects have a large contribution to the nonlinear refractive index. The heat released in the AO10: PAA gel samples by the focussed Gaussian laser beam causes a migration of the solutes in the PAA gel matrix (water and dye molecules) from the hotter region to the colder one.

For a better understanding of these effects, we have investigated the nonlinear transmittance of the investigated samples in the different concentrations used (0.15 and 0.55 mmol/L) for input power 100 mW ; relaxation-like behavior for nonlinearity was observed. As shown in fig.9, the magnitude of the transmittance decreases by increasing of the dye concentration in the PAA gel since saturation of absorption at any concentration is function on concentration pas unit volume and time..
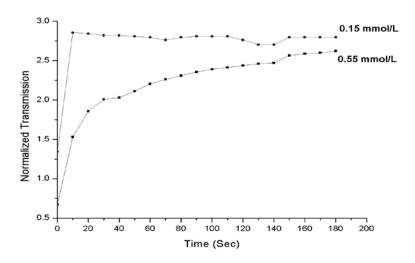
Fig.9. Normalized nonlinear transmission versus time of both concentrations (0.15 mmol/L & 0.55 mmol/L) for input power 100 mWatt.

When a Gaussian beam illuminates a medium, the medium absorbs the light and its temperature rises. The rise in temperature results in a change of refractive index and induces self-diffraction. The formation of a spatial ring pattern is attributed to induced spatial self-phase modulation arising from laser- induced refractive index change and thermal lensing [25]. The large thermal nonlinearity is not only due to the light absorption by AO10 dye but also to the high thermo-optic coefficient and low thermal conductivity of PAA gel [26]. Fig. 10 shows the variation of temperature with time during the course of irradiation for the two concentrations mentioned previously.
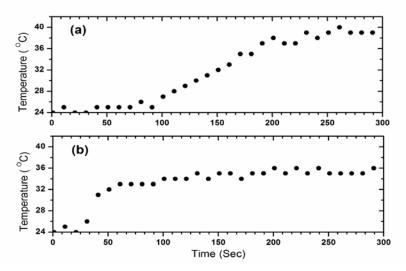

Fig.10. Variation of temperature of the sample versus time for two different concentrations (a: 0.15mmol/L , b: 0.55 mmol/L) and input power 100 mWatt.

8

The nonlinear refractive index of AO10: PAA gel due to thermal heating is strongly governed by the thermal properties of PAA gel used. An important parameter that decides the magnitude of such thermal effects is the thermo-optic coefficient (dn/dT) for PAA gel. The thermal properties of the dye in the matrix are mainly affected on by the matrix, therefore, the heat capacity, C, the density, ρ^*, and the change in thermo-optic coefficient, dn/dT, can be altered by the dye in the matrix [27, 28]. Thus, it can be assumed that a change in the temperature of AO10: PAA gel primarily leads to a change in the density of PAA gel.

The change in thermo-optic coefficient can be determined from the Lorentz-Lorenz relationship [10]. The thermal figure of merit, H, that characterizes the PAA gel is given by $H=(dn/dT)(1/\rho^*.C)$. The PAA gel has a thermal conductivity on the order of 22×10^{-4} W/k.cm which leads to $dn/dT= 1.01\times10^{-4}$ 1/ ^{o}C hence the thermal figure of merit $H=0.45\times10^{-4}$. Thus, the measurement of the thermally induced nonlinear refractive index using thermal self-diffraction technique provides direct estimates for the thermal figure of merit for AO10: PAA gel.

The UV-Vis absorption spectrum of the samples before and after the laser irradiation are the same, indicating that the samples possess good photo-stability (see fig.11). Through the course of observations we can summarise the following. The observed ring pattern behavior is in isomorphism with the interference rings resulted in Michelson interferometer, that is, with increasing the input power a new fringe appears in the shape of full spot that breaks up into a ring with continuously increasing input power and increases in diameter then a new spot appears and so on (see fig. 4(a) and 4 (b)). The increases in the number of diffraction rings and the size of the outermost ring with increasing concentration are due to the increase
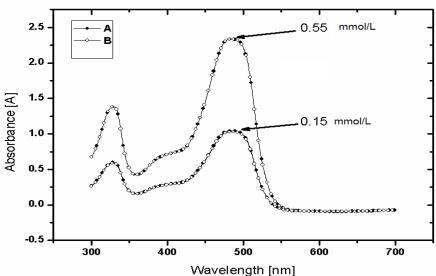

Fig.11. UV–Vis absorption spectrum of two concentrations AO10: PAA gel of (0.15 mmol/L and 0.55mmol/L): (A) after the laser irradiation, and (B) before the laser irradiation.

in the aggregation of the dye molecules at the point of focus at higher concentrations. The diffusivity extends to a large region, thereby causing more interference to take place leading to an increased number of rings. The effect of increasing concentration on the number of rings N is clear when comparing fig. 4 with fig. 5. The number of rings changes from four to five, fig.4 (c,d), over the same power increase it takes to change from five to nine, fig.5c and 5d, that the increase is not linear. The obtained results agree well with those of Ogusu et al [10], Gu et al [12] and Vinitha et al [29], which were obtained in various materials. The comparison

between the experimental and theoretical results shows reasonable agreement.

According to the previously mentioned results, nonlinearity appeared or possibly attributed to the thermal effect, that is, the refractive index increases with increasing input power that appears in the shape of increasing number of rings.

6. Conclusions

Thermal effects appeared to enhance nonlinearities in AO10: PAA gel under pumping with low power visible continuous waveform light from a solid- state diode laser. These effects appeared in the shape of diffraction rings that increased in the number with the increase of input power as well as concentration of the medium. The increase in number of rings is not linear. In the PAA gel samples, due to the thermally induced mechanism, relaxation-like behavior for nonlinearity was observed.

Theoretical result given based on the wave theory of light propagation in nonlinear medium shows some reasonable agreement with the experimental one. The absorption spectral behaviour of each sample shows no drastic changes to occur after the experiment indicating that no permanent changes occur (i.e. the samples possess good photo-stability). These results show that AO10: PAA gel is a promising candidate for nonlinear optical applications.

References

[1] A. S. Zolot'ko, V. F. Kitaeva, N. Kroo, N. N. Sobolev, and L. Csillag, The effect of an optical field on the

nematic phase of the liquid crystal OCBP, JETP Lett. 32,158-161(1980).

[2] A. S. Zolot'ko, V. F. Kitaeva, N. Kroo, N. N. Sobolev, and L. Csillag, Light-induced Freedericksz transition

in an MBBA crystal, JETP Lett. 34, 250-254(1981).

[3] A. S. Zolot'ko, V. F. Kitaeva, N. Kroo, N. N. Sobolev, A. P. Sukhorukov, and L. Csillag, Nature of the

aberration pattern formed as the result of self-focusing of a light beam caused by reorientation of the director

in liquid crystal, Sov.Phys.JETP 56, 786-790(1982).

[4] A. S. Zolot'ko, V. F. Kitaeva, A.V. Kuyumchyan , N. N. Sobolev and A. P. Sukhorukov, Light-induced

second-order phase transition in a spatially bounded region of a nematic liquid crystal, Sov.Phys.JETP 36,

80-83(1982).

[5] A. S.N Zolot'ko, V. F Kitaeva., N. N. Sobolev, V. Yu. Fedorovich and N. M. Shtykov, Photoinduced

periodic grating in cholesteric liquid crystals, Sov.Phys.JETP 32, 614-617(1986).

[6] A. S. Zolot'ko and A. P. Sukhorukov, Freedericksz transition induced in nematic liquid crystal by circularly

polarized light wave, Sov.Phys.JETP 52, 62-65(1990).

[7] A. S. Zolot'ko and V. F. Kitaeva, Light-induced reorientation of a smectic liquid crystal with memory,

Sov.Phys.JETP 50, 33-38(1994).

[8] A. S. Zolot'ko and V. F. Kitaeva, Quasiperiodic structures in multicomponent mixtures of nematic liquid

crystals in the region of the nematic liquid crystal-isotropic liquid phase transition, Sov.Phys.JETP 62, 124-129(1995).

[9] O. Werner, B. Fischer and A. Lewis, Strong self-defocusing effect and four-wave mixing in

bacteriorhodopsin films, Optics Lett.17, 241-234(1992).

[10] K.Ogusu,Y.Kohtani and H.Shao, Laser-induced diffraction rings from an absorbing solution, Opt. Rev.

3(4), 232–234(1996).

[11] E. Brasselet and T. V. Galstian, Optical multistability and confined orientational states in nematic liquid crystals: strong excitation regime, JOSA B 18, 982-988(2001).

[12] Y.Z Gua, Z.J Lianga and F.X Gana, Self-diffraction and optical limiting properties of organically modified sol–gel material containing palladium-octaisopentyloxy-phthalocyanine under cw laser illumination, Opt. Mat.17 (2001) 471-475.

[13] X. Yang , S. Qi, C. Zhang, K. Chen, X. Liang, G. Yang, T. Xub, Y. Han and J.O Tian, The study of self-diffraction of mercury dithizonate in polymer film, Opt. Com. 256, 414-421(2005).

[14] A. Dubietis, P. Polesana, G. Valiulis, A. Stabinis, P. Di Trapani, and A. Piskarskas, Axial emission and spectral broadening in self-focusing of femtosecond Bessel beams, Opt. Exp.15, 4168-4175(2007).

[15] C. Sun, C. Barsi, and J. W. Fleischer, Peakon profiles and collapse-bounce cycles in self-focusing spatial beams, Opt. Exp.16, 20676-20686(2008).

[16] L. Lévesque and R. G. Sabata, Thermal lensing investigation on bulk ceramics and thin-film PLZT using visible and far-infrared laser beams, Opt. Mat. 33, 460-465(2011).

[17] M. Sheik-bahae, A. A. Said, and E. W. Van Stryland, High-sensitivity, single-beam n_2 measurements, Opt. Lett., 14955-957(1989).

[18] G. Vinitha, A. Ramalingam, P.K. Palanisamy, Nonlinear studies of Pararosanilin dye in liquid and solid media, Spect. Acta Part A: Mol. and Biom. Spec 68, 1-5(2007).

[19] Q.M. Ali and P.K.Palanisamy, Investigation of nonlinear optical properties of organic dye by z-scan technique using He–Ne laser, Optik 116, 515-520(2005).

[20] K. Milanchian, H. Tajalli, A. Ghanadzadeh Gilani and M.S. Zakerhamidi, Nonlinear optical properties of two oxazine dyes in aqueous solution and polyacrylamide hydrogel using single beam Z-scan, Opt. Mat. 32, 12–17(2009).

[21] A. B. Villafranca and K. Saravanamuttu, Diffraction rings due to spatial self-phase modulation in a photopolymerizable medium, J. Opt. A: Pure Appl. Opt. 11, 125-202(2009).

[22] S. A. Jenekhe, W. Chen, S. Lo, and S. R. Flom, Large third-order optical nonlinearities in organic polymer superlattices, Appl. Phys. Lett. 57, 126-128(1990).

[23] G.I. Stegeman. In Nonlinear Optics of Organic Molecules and Polymers.Edited by H.S.Nalwa and S.Miyata. CRC Press, Boca Raton (1996).

[24] S. Chávez-Cerda, C. M. Nascimento, M. A. R. C. Alencar, M. G. A. da Silva, M. R. Meneghetti and J. M. Hickmann, Experimental observation of the far field diffraction patterns of divergent and convergent beam in a self-defocusing medium, Annals of Optics, XXIX ENFMC, 1-4(2006).

[25] A. Y. Al-Ahmad, G. M. Shabeeb, A. Q. Abdullah and K. M. Ziadan, Z-scan measurement for the nonlinear absorption and the nonlinear refraction of poly1,4-diazophenylene-bridged-tris(8-hydroxy-quinoline) aluminum (PDPAlq3), Optik 122, 1885–1889(2011).

[26] Z. Mao, L. Qiao, F. He, Y. Liao, C. Wang, Y. Cheng, Thermal-induced nonlinear optical characteristics of ethanol solution doped with silver nanoparticles, Chin. Opt. Lett. 7, 949-952(2009).

[27] F. P. Schafer, Dye Lasers, Springer, Berlin, 1973.

[28] R. W. Boyd, Nonlinear Optics, Academic, San Diego, CA, (2008).

[29] G. Vinitha and A. Ramalingam, Single-beam Z-scan measurement of the third-order optical nonlinearities

of triarylmethane dyes, Laser Phys. 18, 1176-1182(2008).

دراسة عملية ونظرية لانموذج حيود محتث بالليزر في هلام البولي أكريل أميد المشوب بصبغة الحمض البرتقالي العاشر

حسن عبد الله سلطان , حسين علي بدران , علاء ياسين الاحمد و جاسب عبد الحسين مشاري

قسم الفيزياء/ كلية التربية / جامعة البصرة

البصرة – العراق

الخلاصة:

في هذا البحث لاحظنا ودرسنا حلقات الحيود في هلام البولي أكريل أميد المشوب بصبغة الحمض البرتقالي العاشر باستخدام حزمة ليزر مرئية مستمرة . زاد عدد الحلقات بشكل اسي تقريبا مع زيادة كل من قدرة الدخل لحزمة الليزروتركيز الصبغة في الهلام . لقد تم حساب التغير في معامل الانكسار(Δn= 0.004788) ومعامل الانكسار اللاخطي (n_2 cm^2/Watt =10^{-5}) وتغير المعامل الحراري البصري(dn/dT = 1.01×10^{-4} 1/^{o}C) ومعامل الاداء (W=13.7) وكذلك معامل الاداء الحراري ($H = 0.45\times10^{-4}$) . تم حساب قيم معامل الانكسار اللاخطي اعتمادا على عدد الحلقات الناتجة بفعل الحيود الذاتي لحزمة الليزر المار عبر الهلام . ان قيم المعاملات البصرية اللاخطية العالية تعزى الى التاثيرات الناتجة بفعل تسخين العينة نتيجة امتصاص حزمة الليزر المستمر مما يولد تاثيرا حراريا موضعيا يعمل على ظهور حلقات الحيود الذاتي في المادة قيد الدراسة . لقد تمت محاكات النتائج العملية نظريا مستندين الى انموذج نظري ينتج حلقات حيود استنادا الى نظرية الموجة.